

On the slip-weakening behavior of rate- and state dependent constitutive laws

Massimo Cocco and Andrea Bizzarri

Istituto Nazionale di Geofisica e Vulcanologia, Roma, Italy

Received 29 August 2001; revised 26 December 2001; accepted 18 January 2002; published 8 June 2002.

[1] We study the dynamic traction behavior within the cohesive zone during the propagation of earthquake ruptures adopting rate- and state-dependent constitutive relations. The resulting slip-weakening curve displays an equivalent slip-weakening distance (D_0^{eq}), which is different from the parameter L controlling the state variable evolution. The adopted constitutive parameters (a , b , L) control the slip-weakening behavior and the absorbed fracture energy. The dimension of the nucleation patch scales with L and not with D_0^{eq} . We propose a scaling relation between these two lengthscale parameters which prescribes that $D_0^{eq}/L \sim 15$. **INDEX TERMS:** 7209 Seismology: Earthquake dynamics and mechanics; 7215 Seismology: Earthquake parameters; 7260 Seismology: Theory and modeling

1. Introduction

[2] The study of the initiation, propagation and arrest of a dynamic earthquake rupture requires the solution of the elastodynamic equation and the choice of a fault constitutive law, which relates the total dynamic traction to fault friction. In the literature different constitutive laws have been proposed that can be grouped in two main classes: slip-dependent [Barenblatt, 1959; Ida, 1972; Palmer and Rice, 1973; Andrews, 1976a, 1976b; Ohnaka and Yamashita, 1989] and rate- and state-dependent laws [Okubo and Dieterich, 1986; Dieterich, 1979]. The former assumes that friction is a function of the fault slip only, while the latter implies that the friction is a function of slip velocity and state variables [Ruina, 1983]. The state variable provides a memory of previous slip episodes and its evolution equation guarantees a time dependence of friction. Because rate- and state-dependent (R&S) laws imply fault restrengthening after the dynamic failure, they can be used to simulate repeated seismic cycles [Rice, 1993]. Slip-dependent laws have been widely used in seismology to model the dynamic rupture propagation and the emission of seismic waves during a single large magnitude earthquake [Day, 1982; Olsen et al., 1997, among different others]. In the classic form of slip-weakening (SW) law [see Andrews, 1976a, 1976b] the total traction is a function of the yield stress (τ_u), the kinetic friction level (τ_f) and the characteristic SW distance D_0 (the slip required for stress to drop, see Figure 1). A slip-dependent constitutive behavior has been also inferred in laboratory experiments [see Okubo and Dieterich, 1984; Ohnaka and Shen, 1999].

[3] In the following of the paper, we refer to the cohesive zone (or breakdown zone) as the zone of shear stress degradation near the crack tip of a propagating dynamic rupture front. The breakdown processes are those phenomena occurring within the cohesive zone responsible for the fracture energy absorption and the slip acceleration. They are the most important phenomena that have to be correctly reproduced for those investigations aimed to model the dynamic rupture propagation during a single earthquake. For these purposes the adoption of a classic SW law is quite convenient because it specifies the yield stress, the kinetic friction level and the

critical SW distance (see Figure 1). This means that the traction behavior within the cohesive zone is assigned “a priori”. Several authors have proposed that R&S friction laws imply a traction dependence on slip [Okubo, 1989; Beeler and Tullis, 1996; Dieterich and Kilgore, 1996]. However, in the framework of the R&S formulation the yield stress and the kinetic friction within the cohesive zone depend on slip rate and state; they are not assigned, and therefore unknown “a priori”. This implies that R&S constitutive laws cannot be easily used to simulate the dynamic rupture propagation with a prescribed traction evolution. We point out that the R&S friction formulation does not explicitly include an analytical traction dependence on slip. The goal of this study is to discuss the SW behavior within the cohesive zone specific of R&S friction laws during the dynamic rupture propagation.

2. The Adopted Numerical Method

[4] We solve the elastodynamic equation for a 2D in-plane crack using a finite difference (FD) approach [Andrews and Ben-Zion, 1997] and adopting a R&S dependent law with a slowness (ageing) evolution equation. Bizzarri et al. [2001] presented a detailed comparison between solutions of the elastodynamic equation and discuss the required stability and convergence criteria to be satisfied to have enough resolution to investigate the processes occurring within the cohesive zone. We refer to that paper for an extensive presentation of the adopted numerical procedure. Among the different analytical formulations of R&S constitutive laws, we use in this study the following equations:

$$\begin{aligned} \tau(V, \Psi) &= \tau_* - a\sigma_n \ln\left(\frac{V}{V_*} + 1\right) + b\sigma_n \ln\left(\frac{\Psi V_*}{L} + 1\right) \\ \frac{d\Psi}{dt} &= 1 - \frac{\Psi V}{L} \end{aligned} \quad (1)$$

where τ_* , V_* are arbitrary reference values of friction and slip velocity, respectively, and a , b and L are the constitutive parameters. Ψ is the state variable that has the meaning of an average contact time between the sliding surfaces. Figure 1 shows an example of numerical simulation obtained using this constitutive formulation with our FD numerical method and assuming the same procedure for fault nucleation described in Bizzarri et al. [2001].

3. Dynamic Traction Behavior Within the Cohesive Zone

[5] Figure 1 shows that in a homogeneous configuration using a R&S constitutive formulation the cohesive zone shrinks during the dynamic rupture propagation, as also pointed out for the classic SW law [Andrews, 1976a, 1976b]. The resulting time histories of slip, slip velocity and total dynamic traction are, as expected, very similar to those obtained in numerical simulations which adopt the classic SW laws [see comparisons in Bizzarri et al., 2001]. However, the analysis of total dynamic traction as a function of slip velocity and slip reveals that velocity-hardening

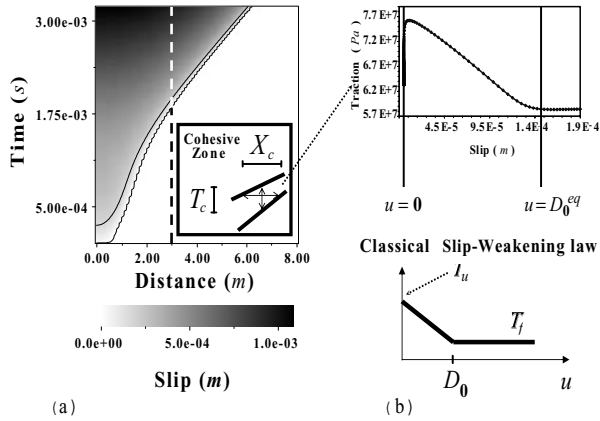


Figure 1. (a) Spatio-temporal evolution of slip for a 2D in-plane crack: The gray scale shows the slip amplitudes as a function of time and spatial position. The black lines depict the cohesive zone where the total dynamic traction drops from the maximum yield stress to the kinetic friction (as shown in (b) for a point located at a distance of 3.0 m, dashed line). The box inserted in panel (a) depicts a zoom of the cohesive zone: T_c is the duration and X_c is the spatial extension of the cohesive zone. A SW behavior occurs within the cohesive zone also when a R&S constitutive law is adopted and it results very similar to the classical theoretical law (see panel b). The adopted constitutive parameters are: $\lambda = \mu = 27$ GPa, $V_p = 5196$ m/s, $V_S = 3000$ m/s, $\mu_* = 0.56$, $\sigma_n = 100$ MPa, $a = 0.012$, $b = 0.016$, $L = 10$ μm , $V_i = 10$ $\mu\text{m/s}$. They represent the reference configuration for all simulations presented in this paper.

and -weakening clearly exist, and the resulting SW curves are very similar to the generally adopted classic laws (see Figure 2). A characteristic SW distance exists also for the R&S friction formulation [Okubo and Dieterich, 1986]. This is not surprising because the slip increase occurs while total dynamic traction decreases yielding slip-weakening. The important question is what controls the SW behavior in the R&S formulation. Our numerical simulations show that, when the propagating rupture front approaches the target grid point, the dynamic stress increases due to the direct effect of friction, although the growth of slip velocity is quite slow at the beginning (phase I in Figure 2). When the dynamic traction is reaching its maximum value (the yield stress) the slip velocity suddenly increases (phase II); this acceleration phase begins when the total dynamic traction is close to the peak yield stress. The subsequent traction drop coincides with the SW phase and slip velocity reaches its maximum value (phase III). The acceleration from the initial to the peak slip velocity is very fast and occurs in an extremely short time. Finally, the dynamic traction reaches the kinetic friction level and slip velocity decreases to the new steady state value. The analysis of the 3D phase trajectories represented in Figure 3 shows that SW occurs when the acceleration stage is already started. It is the evolution of the state variable within the cohesive zone that drives the slip acceleration and the fast approaching to the peak slip velocity. This evolution occurs within the cohesive zone when the rupture propagation is initiated and fully dynamic; it has nothing to do with the nucleation process and it happens well before of the eventual healing phases. It is clear that during the dynamic slip the total traction depends on slip, slip velocity and the state variable [Madariaga and Cochard, 1996], although the adopted constitutive formulation only requires the analytical dependence on slip velocity and state. Several authors adopted a rate- and slip-weakening friction in a theoretical way [Madariaga et al., 1998; Fukuyama and Madariaga, 1998]. We have shown, however, that hardening effects clearly exist and the state variable evolution controls the traction behavior and the slip acceleration.

[6] Our numerical results confirm the findings of previous studies [Okubo, 1989; Guatteri et al., 2001] but rise new questions and stimulating considerations. SW is intrinsic in R&S laws, but the characteristic SW distance does not coincide with L , which is the characteristic length parameter of this dynamic formulation. We define this slip-weakening distance resulting from R&S laws as an equivalent value D_0^{eq} . The fast evolution of slip velocity represents a serious limitation to retrieve and constrain the constitutive behavior and parameters within the cohesive zone by inverting recorded seismograms [see Guatteri et al., 2001]. Attempts in constraining the critical SW distance by means of dynamic consistent waveform inversions [Ide and Takeo, 1997; Guatteri and Spudich, 2000], as well as forward 3D dynamic modeling [Olsen et al., 1997], yield values larger than 0.2 m. We do not discuss here the required resolution to constrain the SW distance from recorded seismograms. We point out, however, that these large values might be caused by smearing effects due to the lack of resolution of the cohesive zone dimension. Moreover, if these large values are real, they would imply nucleation patches ranging between few to tens of kilometers, sometimes reaching 50% of the whole fault length [see for instance Voisin et al., 2001]. We have performed many numerical simulations using different values of L and keeping constant the others constitutive parameters. The results of these calculations are shown in Figure 4. The SW curves plotted in this figure point out the dependence of D_0^{eq} on L : the equivalent SW distance resulting from the R&S dependent law here considered is larger than the adopted L value and it increases for increasing L . Moreover, we emphasize that D_0^{eq} also depends on the other constitutive parameters a and b , since they control the yield stress and the kinetic friction. This latter result is not discussed here in detail because it requires an extensive presentation.

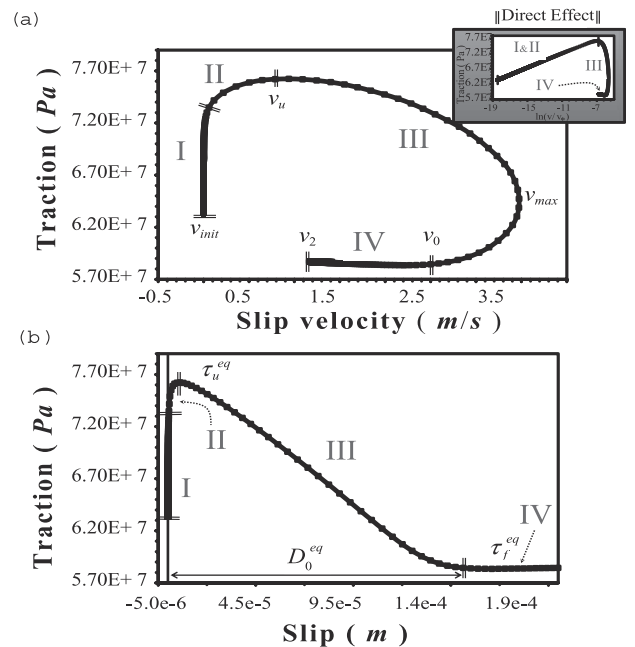


Figure 2. Total dynamic traction as a function of slip velocity (a) and slip (b). The first two stages (I and II) correspond to the slip- and the velocity-hardening behavior. The fast slip acceleration (II and III) occurs when the dynamic traction approaches the yield stress and therefore drops to the kinetic friction level (τ_f). D_0^{eq} is the equivalent slip-weakening distance. The box in the upper left corner of (a) shows the total dynamic traction (in a log scale) as a function of the $\log(V/V_*)$.

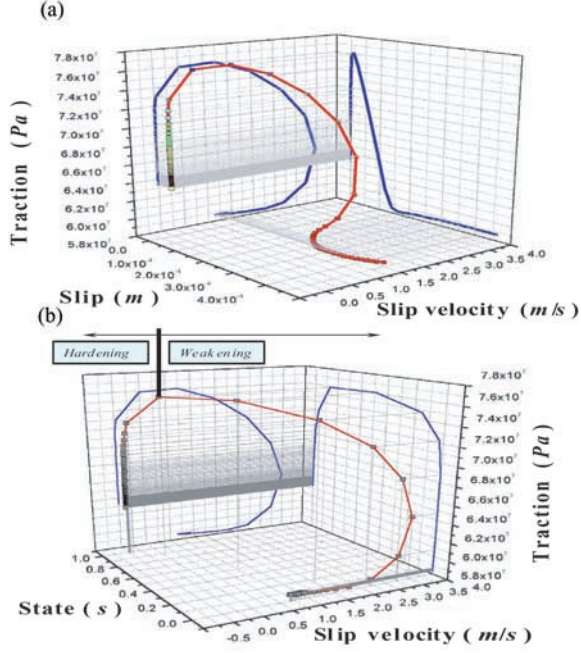


Figure 3. 3D phase diagrams showing total dynamic traction as a function of slip and slip velocity (a) and state and slip velocity (b). The projections of the 3D trajectories on the vertical planes show the expected behaviors for slip-weakening, velocity-hardening and -weakening as well as the state variable evolution within the cohesive zone. In (b) the state evolves from the initial steady state (L/V_i) up to the final, new steady state (L/V_0).

3.1. A Scaling Law Between L and D_0^{eq}

[7] Although the friction dependence on slip has been proposed by previous authors in the framework of the R&S dependent laws, it has not been analytically formulated, at least in a feasible way to represent the traction behavior within the cohesive zone. Assuming a nearly constant slip velocity [Dieterich and Kilgore, 1996], the traction depends on the state variable only and the dependence on slip can be easily derived. However, such an assumption is certainly not valid to represent the processes occurring within the cohesive zone, where slip velocity is very different from being constant. Our simulations clearly point out that the state variable evolves within the cohesive zone from its initial value to a new steady state value (Figure 3). This evolution controls both the friction increase and decrease and the consequent slip acceleration and it involves proportionality between D_0^{eq} and L . In order to obtain a scaling relation between these length parameters, we assume that the initial and final steady-state values of the state variable are $\Psi_i^{ss} = L/V_i$, and $\Psi_0^{ss} = L/V_0$, respectively. Here, V_i and V_0 are the initial velocity and its final steady-state value [see Figure 2]. If slip velocity is large enough to assume that $1/V$ is negligible, therefore the integration over slip of the evolution equation gives $\Psi = (L/V) \exp(-\Delta u/L)$. When $\Delta u = D_0^{eq}$ we have that $\Psi = \Psi_i^{ss}$ and therefore we can easily derive the following relation: $D_0^{eq} = L \ln(V_0/V_i)$. By substituting these relations in the steady-state equation for friction, we can derive a relation between the logarithm of the velocity ratio and the dynamic stress drop $\ln(V_0/V_i) \cong (\tau_u^{eq} - \tau_f^{eq})/(b\sigma_n)$, which yields

$$D_0^{eq} = L \ln\left(\frac{V_0}{V_i}\right) \approx \frac{\tau_u^{eq} - \tau_f^{eq}}{b\sigma_n} L \quad (2)$$

where τ_u^{eq} and τ_f^{eq} represent the yield and the kinetic stress values for the R&S constitutive formulation. The proportionality factor

between these two length parameters scales with the dynamic stress drop ($\tau_u^{eq} - \tau_f^{eq}$) and the constitutive parameters. The dependence on L is quite simple, but the effect of the other constitutive parameters a and b is more complex since they also affect the yield stress and the kinetic friction. The theoretical relation proposed above shows that the equivalent SW distance D_0^{eq} depends on the initial value of slip velocity, which controls the initial steady-state value of the state variable. The proposed scaling between D_0^{eq} and the dynamic stress drop ($\tau_u^{eq} - \tau_f^{eq}$) is an approximated relation: the calculated D_0^{eq} values slightly underestimate those resulting from numerical simulations. Because the initial slip velocity is totally arbitrary, it is difficult in the framework of R&S formulation to prescribe the traction evolution and the SW behavior within the cohesive zone. We can only infer an approximated value of the equivalent slip-weakening distance from the proposed scaling law. Moreover, the difference between D_0^{eq} and L depends on the adoption of a slowness (ageing) evolution equation. Preliminary results indicate that a slip evolution equation does not provide similar values for D_0^{eq} and the scaling with L is different; however, further investigations are needed to explain and interpret this different behavior.

4. Discussion and Conclusive Remarks

[8] In our simulations we have used values of the L parameter derived from laboratory experiments ($L \sim 1 \div 10 \mu\text{m}$), which yield D_0^{eq} values of the order of $0.02 \div 0.2 \text{ mm}$. These values are much smaller than those obtained by waveform inversions which suggest $D_0^{eq} \sim 0.2 \div 0.5 \text{ m}$. Guatteri *et al.* [2001] estimated the L parameter from strong motion recordings of the 1995 Kobe earthquake, and their L values range between 1 to 5 cm assuming the SW distance inferred by Ide and Takeo [1997]. Our numerical simulations yield a D_0^{eq}/L ratio nearly equal to 15. Assuming $L \sim 1 \text{ cm}$ [Scholz, 1988] for actual fault dimensions, the proposed scaling law yields D_0^{eq} values very close to 0.2 m, in agreement with the results of Guatteri *et al.* [2001]. If $D_0^{eq} \sim 0.2 \text{ m}$ is a believable result, the problem is therefore to scale the parameter L from laboratory to actual fault dimensions. If the lengthscale L of rate and state effects has the multi-micron scale of contacting asperities along surfaces, it can hardly be related to D_0^{eq} . The latter may be associated to different weakening processes (such as thermal weakening) occurring at high slip rates. On the contrary, we may assume that reasonable values of L for actual faults are close to the centimeter scale due to the presence of fault gouge

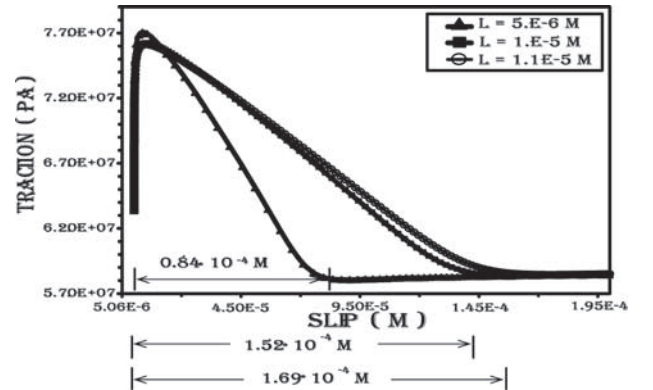


Figure 4. SW curves for different values of the parameter L but keeping constant all the other constitutive parameters and the initial conditions. Increasing L increases the equivalent SW distance, and the latter is always larger than the assumed L value. The yield stress and the kinetic friction level are the same among the three different simulations. As expected the weakening rate decreases for smaller value of the equivalent slip-weakening distance.

responding to high slip velocities [Marone and Kilgore, 1993; Mair and Marone, 1999]. In this latter case, we are allowed to scale our simulations to actual fault dimensions and the proposed scaling law may explain the inferred D_0^{eq} values. Because the nucleation patch scales with L and not with D_0^{eq} , we should expect a much reasonable dimension of the nucleation patch with respect to the whole fault length even for $D_0^{eq} = 0.2$ m.

[9] Another important implication emerging from our results concerns the fracture energy, which scales with D_0^{eq} and not explicitly with the parameter L . This implies that, in the framework of R&S laws, the evolution of the state variable controls the traction drop and causes a finite fracture energy to be absorbed within the cohesive zone. In this context this apparent fracture energy depends in a complex way on the adopted constitutive parameters (a , b and L). The values of a and b affect the yield stress and the kinetic friction value, and the fracture energy depends on the behavior of friction assumed at high slip rate. These results confirm that is the combination of constitutive parameters rather than their individual values that controls the rupture dynamics. Our estimates of fracture energy (G) for the simulations shown in Figure 4 range between 1 and $3 \cdot 10^4$ J/m², in agreement with previous studies [Okubo and Dieterich, 1984]. Scaling these values to actual fault dimensions yield a fracture energy of the order of 10^7 J/m², which is still in agreement with previous estimates [see Guatteri et al., 2001 and references therein].

[10] The results presented here further support the importance and the benefit of using R&S dependent constitutive laws to model fault and earthquake mechanics. This constitutive formulation implies a SW behavior during the fully dynamic rupture propagation, which is not assigned “a priori” and spontaneously evolves depending on the adopted constitutive parameters. There is no need to assume that friction must become independent of slip velocity at high speeds to resemble SW. Our results show that SW is a characteristic behavior of R&S constitutive laws during the dynamic rupture growth and that this constitutive formulation contains a physical control of the breakdown processes occurring within the cohesive zone. This is in agreement with the results of “stick-slip” laboratory experiments, which have been interpreted either as rate and state [Dieterich, 1979; Okubo and Dieterich, 1986] or slip-dependent friction [Ohnaka et al., 1987]. However, the friction behavior at high slip rates affects the fracture energy absorbed within the cohesive zone. Our results could also be interpreted in the perspective of a unified constitutive formulation, at least for the dynamic slip episodes. While this can be a likely expectation for the dynamic rupture growth, this is certainly not true for the nucleation process. Earthquake nucleation is described in a different way by these two constitutive formulations [Dieterich, 1992; Shibazaki and Matsu'ura, 1998], which have both been proposed to model stick-slip episodes.

[11] **Acknowledgments.** Conversations with Joe Andrews and the availability of its 2D code stimulated and motivated this study. We thank Alain Cochard Raúl Madariaga, Stefan Nielsen, Paul Spudich and Jim Rice who reviewed a preliminary version of the paper and two anonymous referees who improved the text with their criticism.

References

- Andrews, D. J., Rupture propagation with finite stress in antiplane strain, *J. Geophys. Res.*, *81*, 3575–3582, 1976a.
- Andrews, D. J., Rupture velocity of plane strain shear cracks, *J. Geophys. Res.*, *81*, 5679–5687, 1976b.
- Andrews, D. J., and Y. Ben-Zion, Wrinkle-like slip pulse on a fault between different materials, *J. Geophys. Res.*, *102*, 553–571, 1997.
- Barenblatt, G. I., Concerning equilibrium crack forming during brittle fracture. The stability of isolated cracks. Relationship with energetic theories, *Appl. Math. Mech.*, *23*, 1273–1282, 1959.
- Beeler, N. M., and T. E. Tullis, Self-healing slip pulses in Dynamic rupture models due to velocity-dependent strength, *Bull. Seism. Soc. Am.*, *86*, 1130–1148, 1996.
- Bizzarri, A., M. Cocco, D. J. Andrews, and E. Boschi, Solving the dynamic rupture problem with different numerical approaches and constitutive laws, *Geophys. J. Int.*, *144*, 656–678, 2001.
- Day, S. M., Three-dimensional finite difference simulation of fault dynamics: Rectangular faults with fixed rupture velocity, *Bull. Seism. Soc. Am.*, *72*, 705–727, 1982.
- Dieterich, J. H., Modeling of rock friction-1. Experimental results and constitutive equations, *J. Geophys. Res.*, *84*, 2161–2168, 1979.
- Dieterich, J. H., Earthquake nucleation on faults with rate- and state-dependent strength, *Tectonophysics*, *211*, 115–134, 1992.
- Dieterich, J. H., and B. Kilgore, Implications of fault constitutive properties for earthquake prediction, *Proc. Natl. Acad. Sci. USA*, *93*, 3787–3794, 1996.
- Fukuyama, E., and R. Madariaga, Rupture dynamics of a planar fault in a 3-D elastic medium: Rate- and slip-weakening friction, *Bull. Seism. Soc. Am.*, *88*, 1–17, 1998.
- Guatteri, M., and P. Spudich, What can strong-motion data tell us about slip-weakening fault-friction laws?, *Bull. Seism. Soc. Am.*, *90*, 98–116, 2000.
- Guatteri, M., P. Spudich, and G. C. Beroza, Inferring rate and state friction parameters from a rupture model of the 1995 Hyogo-ken Nambu (Kobe) Japan earthquake, *J. Geophys. Res.* in press, 2001.
- Ida, Y., Cohesive force across the tip of a longitudinal-shear crack and Griffith's specific surface energy, *J. Geophys. Res.*, *77*, 3796–3805, 1972.
- Ide, S., and M. Takeo, Determination of constitutive relations of fault slip based on seismic wave analysis, *J. Geophys. Res.*, *102*, 27,379–27,391, 1997.
- Madariaga, R., and A. Cochard, Dynamic friction and the origin of the complexity of earthquake sources, *Proc. Natl. Acad. Sci. USA*, *93*, 3819–3824, 1996.
- Madariaga, R., K. B. Olsen, and R. Archuleta, Modeling dynamic rupture in a 3D earthquake fault model, *Bull. Seism. Soc. Am.*, *88*, 1182–1197, 1998.
- Marone, C. J., and B. Kilgore, Scaling of the critical slip distance for seismic faulting with shear strain in fault zones, *Nature*, *362*, 618–621, 1993.
- Mair, K., and C. J. Marone, Friction of simulated fault gouge for a wide range of velocities and normal stresses, *J. Geophys. Res.*, *104*, 28,899–28,914, 1999.
- Ohnaka, M., Y. Kuwahara, and K. Yamamoto, Constitutive relations between dynamic physical parameters near a tip of the propagating slip zone during stick-slip shear failure, *Tectonophysics*, *144*, 109–125, 1987.
- Ohnaka, M., and T. Yamashita, A cohesive zone model for dynamic shear faulting based on experimentally inferred constitutive relation and strong motion source parameters, *J. Geophys. Res.*, *94*, 4089–4104, 1989.
- Ohnaka, M., and L. F. Shen, Scaling of the shear rupture process from nucleation to dynamic propagation: Implications of geometric irregularity of the rupturing surfaces, *J. Geophys. Res.*, *104*, 817–844, 1999.
- Okubo, P. G., and J. H. Dieterich, Effects of physical fault properties on frictional instabilities produced on simulated faults, *J. Geophys. Res.*, *89*, 5817–5827, 1984.
- Okubo, P. G., and J. H. Dieterich, State variable fault constitutive relations for dynamic slip, *Earthquake Source Mechanics*, Geophysical Monograph, *37*, Maurice Ewing Series, 6, edited by S. Das, J. Boatwright and C. H. Scholz, pp. 25–35, 1986.
- Okubo, P. G., Dynamic rupture modeling with laboratory-derived constitutive relations, *J. Geophys. Res.*, *94*, 12,321–12,335, 1989.
- Olsen, K. B., R. Madariaga, and R. J. Archuleta, Three-dimensional dynamic simulation of the 992 Landers earthquake, *Science*, *278*, 834–838, 1997.
- Palmer, A. C., and J. R. Rice, The growth of slip surfaces in the progressive failure of overconsolidated clay, *Proceedings of the Royal Society of London*, Vol. A332, 527–548, 1973.
- Rice, J. R., Spatio-temporal complexity of slip on a fault, *J. Geophys. Res.*, *98*, 9885–9907, 1993.
- Ruina, A. L., Slip instability and state variable friction laws, *J. Geophys. Res.*, *88*, 10,359–10,370, 1983.
- Scholz, C. H., Earthquakes and friction laws, *Nature*, *336*, 37–42, 1988.
- Shibazaki, B., and M. Matsu'ura, Transition process from nucleation to high-speed rupture propagation: Scaling from stick-slip experiments to natural earthquakes, *Geophys. J. Intl.*, *132*, 14–30, 1998.
- Voisin, C., M., Campillo, I. R., Ionescu, F. Cotton, and O. Scotti, Dynamic versus static stress triggering and friction parameters: Inferences from the November 23, 1980 Irpinia earthquake, *J. Geophys. Res.*, 2001.